ADAPTIVE DESIGN OF COSTAS RADAR SIGNAL WITH IMPROVED NARROWBAND AMBIGUITY FUNCTION

Ramez EIZDASHIRE ALI DEEP[1], Radwan KASTANTIN[2]

In this paper we propose to incorporate scattering coefficients of a target into weighted Costas waveform model and using adaptive technique to find these optimal weights, and hence to improve the radar's Narrowband Ambiguity Function (NAF). We confirm that the proposed formula of NAF is considered as a better representation of the target echo and results in much better Auto-Correlation Function (ACF) in the sense of decreasing the sidelobe level without needing to increase the number of the frequencies in the Costas waveform. We will also show that the obtained adaptive waveform doesn't affect the original resolution and yields less sensitivity to delay-Doppler coupling problem. We suppose that the received signal depends on scattering coefficients obtained from Swerling models. The developed optimization problem, to adaptively design the weighted Costas waveform, adequately describe the features of the target such that the volume under the corresponding NAF surface best approximates the volume under a desired ambiguity function (AF) surface. What is more, we demonstrate that the optimal solution will redistributes the signal energy at scatters of the target such that the weaker scatter should be assigned with more energy than the stronger one. Finally, we will prove the effectiveness of our adaptive waveform design through simulation results.

Keywords: Adaptive Waveform Design, Optimization Problem, Scattering Coefficients, Swerling models, Costas Chirp Signal, Ambiguity Function

1. Introduction

The art of designing radar waveform depends mostly on both the experiences and expertise of the designers in catching the suitable waveform. These experiences are obtained by manipulating signal parameters, using special building blocks with desirable mathematical properties [1]. One of the main goals in radar system design is to suitably select the transmit waveform, because the waveform of the transmitted signal controls the delay-Doppler resolution, the detection performance in the presence of noise and/or masking clutters [1][2][3][4]. Numerous modern literature reviews are rich of ideas concentrating on optimal adaptive waveform design to improve the radar system performance. Wei Fu, *et al* propose an adaptive optimal waveform design algorithm that maximizes the signal-to-interference-plus-noise ratio at the receiver output, and

[1] MSc Student, Department of Communication- Higher Institute of Applied Sciences and Technology, Damascus, Syria, email: ramez.alideep@hiast.edu.sy

[2] Professor - Department of Communication- Higher Institute of Applied Sciences and Technology, Damascus, Syria, email: Radwan.Kastantin@hiast.edu.sy

their design is based on using a frequency-stepped chirp signal with arbitrary sub-pulse bandwidths and chirp slopes [5]. Their optimization problem includes three constraints; the integral sidelobe level of an autocorrelation function, the energy, and the peak-to-average power ratio. The effectiveness of their designed waveform when compared with a linear frequency modulation signal, results in a great improvement in the target detection performance. Peng Chen, *et al* study the estimation of target scattering coefficients in an adaptive radar system. They propose a novel estimation method based on Kalman filter (KF) with waveform optimization for the temporally correlated with both noise and clutter [6]. The proposed adaptive waveform design is based on a direct optimization method subject to the practical constraints including the transmitted energy, the peak-to-average power ratio, and the target detection performance. The proposed KF-based method with waveform optimization can obviously improve the estimation performance [6]. David A. Hague uses Multi-Tone Sinusoidal Frequency Modulation (MTSFM) to get an optimal waveform design based on adapting the Fourier Series coefficients of MTSFM waveform's modulation function [7]. Hague 's representation results in a constant amplitude waveform with a continuous modulation function whose spectrum, Auto-Correlation Function (ACF), and Ambiguity Function (AF) shapes are modified by adapting the Fourier Series coefficients. His adaptive MTSFM waveforms proposed possesses a low Peak-to-Average Power Ratio (PAPR) and high Spectral Efficiency (SE). Xiongjun Fu, *et al* propose a waveform synthesis method for adaptive radar based on using a cascade of the water-filling algorithm and iterative least squares (LS) approach, and the optimal energy spectrum density (ESD) of the synthesized waveform is obtained [8]. Their optimal waveform synthesis method can be considered as competent for adaptive radar. Satyabrata Sen and Arye Nehorai develop an adaptive waveform design based on a multicarrier OFDM signal. They compute the corresponding Wideband Ambiguity Function (WAF) at the output of the Matched Filter (MF) such that the received signal depends on the scattering coefficients of the target [9]. Their optimization procedure selects the OFDM waveform such that the volume of the corresponding WAF best approximates the volume of a desired ambiguity function, and hence the resulting AF along with the associated ACF is improved in the sense of decreasing peak sidelobe level (PSL).

Practical waveform design problem remains a challenging research domain despite numerous attempts to solve it. Radar waveform design has been considered as an important research problem in radar system design since the elegant work of Woodward [10]. Woodward developed the AF and interpreted its surface as a measure of the uncertainty of the delay and Doppler of a returning echo from a target, simultaneously. In fact, the AF surface is usually interpreted as a matched filter response and can be naturally used as a performance measure in radar waveform design [1][10]. Historically speaking, Wilcox proposed a

complete mathematical solution in the LS sense such that the desired AF surface was defined in analytical form [11], which is not the case in any practical radar application for two main reasons: (1) in the set of all possible two-dimensional functions, ambiguity functions are rare, and it is unusual for an arbitrary two-dimensional function to satisfy the mathematical properties of the AF surface, (2) it is mostly not necessary to have a certain shape of the AF surface analytically defined in the entire delay-Doppler plane and to approximate only part of that surface corresponding to a desired subregion in the plane. Sussman approached the problem by approximating a desired AF surface in the LS sense too, but his optimization procedure stretches again over the entire delay-Doppler plane. Hence, the resultant waveform can produce an "all-purpose" AF that would be more or less suitable for any radar applications [12]. I. Gladkova and D. Chebanov extended Wilcox's LS approach by restricting the optimization procedure over some limited subregions in the time-doppler delays plane particularly surrounding the main-lobe of the ambiguity surface [13][14].

In this paper, we propose an adaptive waveform design based on Costas chirp signal [15] for radar application. We compute its Narrowband Ambiguity Function (NAF) formulas of the proposed waveform taking into consideration the effects of the target RCS fluctuation on received signal. Actually, the analysis of detection or recognition of a target has so far assumed that the echo signal has a constant amplitude, which is not always true since the real targets are made up of several scatters, and the net echo depends on the way in which the contributions from these scatters add vectorially, and/or the motion of the target. In our work, we incorporate the scattering coefficients of the target into the reflected echo signal model, and weight the transmit waveform. The motivation for incorporating the target scattering coefficients is that these coefficients can be effectively estimated as Peng Chen, et al suggest in [6]. In the simulation, we will use Swerling models [2] to realize scattering coefficients. Moreover, the motivation for using Costas chirp signal is because of its high delay-Doppler resolution, and we aim to considerably reduce its PSL, and hence obtaining much better ACF than that of normal Costas chirp signal. Costas hopping sequence of length N yields ACF with a maximum height just $1 / N$ times of the main lobe level height [15]. We develop an optimization problem that approximates a desired ambiguity surface in the LS sense in presence of two constraints; one to ensure transmission over all frequencies of Costas signal and the other to meet the signal energy normalization requirement. The solution of the optimization problem introduces an adaptive (optimal) weights with respect to the scattering coefficients of the target. The adaptive weights will redistribute the signal energy such that the weaker scatter should be supplied with more energy than the stronger one. As a result, the adaptive waveform will yield a much better ACF in the sense of PSL reduction without needing to increase N, and without affecting the original

resolution. Moreover, the adaptive waveform will yield less sensitivity to delay-Doppler coupling problem.

2. Signal Model and its corresponding NAF

2.1 Weighted Costas Signal Model

We consider a monostatic radar employing weighted Costas chirp signal whose hopping sequence is $c=[c_0,c_1,...,c_{N-1}]$ with N active subcarriers $\{f_l\}_{0\le l\le N-1}$ (each of duration τ_1 sec and equally spaced by δf Hz) such that $f_l=c_l/\tau_1$ Hz and $\delta f\times\tau_1=1$, a bandwidth of $B=N\delta f$ Hz, and pulse duration of $T=N\tau_1$ sec [15], and hence the Time-Bandwidth product will be $TB=N\tau_1\times N\delta f\times\tau_1=N^2$. $\delta f\times\tau_1=1$ implies orthogonality property in the frequency domain similarly to the OFDM signal model presented in [9]. Costas stated that the delay resolution of such a waveform is τ_1, while the Doppler resolution is $1/T$,[15]. Let $\boldsymbol{a}=[a_0,a_1,...,a_{N-1}]^T$ contains the complex weights transmitted over different subcarriers, satisfying $\sum_{l=0}^{N-1}|a_l|^2=1$ in order to meet the signal energy normalization requirement. Then, the complex envelope of a single pulse can be represented as

$$s(t)=\frac{1}{\sqrt{N\tau_1}}\sum_{l=0}^{N-1}a_l s_l(t-l\tau_1):s_l(t)=\begin{cases}e^{j2\pi f_l t} & 0\le t\le\tau_1\\ 0 & elsewhere\end{cases}. \quad (1)$$

Let f_c be the carrier frequency of operation, then the transmitted signal is given by

$$s_{TX}(t)=Re\left\{s(t)e^{j2\pi f_c t}\right\}. \quad (2)$$

We consider a far-field point target moving at radial velocity v m/s with respect to the radar, and at distance R meters far away from the radar. We suppose that the velocity v is constant during the pulse duration T, and assume that the transmitted radar signal follows a narrow-band signal model. Hence, we can model the echo signal reflected from the radar target while ignoring noise [11] as

$$y_1(t)=s(t-\tau)e^{j2\pi f_d t}, \quad (3)$$

where $\tau=2R/c$ is the time delay of the electromagnetic wave path, c is the velocity of light in the vacuum, and $\tau=2v/\lambda$ is the Doppler shift with $\lambda=c/f_c$ being the wavelength of transmitted wave. Substituting (1) into (3), we get

$$y_1(t)=\frac{1}{\sqrt{N\tau_1}}\sum_{l=0}^{N-1}a_l s_l(t-\tau-l\tau_1)e^{j2\pi f_d t}. \quad (4)$$

However, note that equation (4) does not include any modeling of the target scattering coefficients, so let $\boldsymbol{x}=[x_0,x_1,...,x_{N-1}]^T$ be a complex vector containing the scattering coefficients of the target at different subcarriers, so we incorporate scattering coefficients into the expressions of (4), such that we receive

$$y(t)=\frac{1}{\sqrt{N\,\tau_1}}\sum_{l=0}^{N-1}x_l a_l s_l(t-\tau-l\,\tau_1)e^{j\,2\pi f_d t}\ . \tag{5}$$

2.2 NAF Model of a Weighted Costas Pulse

By analogy with Woodward's definition of ambiguity function, we define the corresponding NAF of both the transmitted waveform (equation (1)) and its received version (equation (5)) as a matched filter (MF) response such that

$$\chi_{MF}(\tau,f_d,\boldsymbol{a},\boldsymbol{x})\ \square\ \int_{-\infty}^{+\infty}s(t)y^*(t)dt\ , \tag{6}$$

where $(.)^*$ denotes the complex conjugate operator. Substituting (1) into (6), we can write

$$\chi_{MF}(\tau,f_d,\boldsymbol{a},\boldsymbol{x})=\frac{1}{N\,\tau_1}\int_{-\infty}^{+\infty}\left[\sum_{l_1=0}^{N-1}a_{l_1}s_{l_1}(t-l_1\tau_1)\right]\left[\sum_{l_2=0}^{N-1}x_{l_2}^*a_{l_2}^*s_{l_2}^*(t-\tau-l_2\tau_1)\right]e^{-j\,2\pi f_d t}dt\ , \tag{7}$$

or

$$\chi_{MF}(\tau,f_d,\boldsymbol{a},\boldsymbol{x})=\frac{1}{N\,\tau_1}\sum_{l_1=0}^{N-1}\sum_{l_2=0}^{N-1}x_{l_2}^*a_{l_2}^*a_{l_1}\int_{-\infty}^{+\infty}s_{l_1}(t-l_1\tau_1)s_{l_2}^*(t-\tau-l_2\tau_1)e^{-j\,2\pi f_d t}dt\ . \tag{8}$$

Now, we define a new function

$$\chi_{s_{l_1}s_{l_2}}(\tau,f_d)=\frac{1}{N\,\tau_1}\int_{-\infty}^{+\infty}s_{l_1}(t-l_1\tau_1)s_{l_2}^*(t-\tau-l_2\tau_1)e^{-j\,2\pi f_d t}dt\ . \tag{9}$$

Hence, the NAF of one radar pulse in our model is

$$\chi_{MF}(\tau,f_d,\boldsymbol{a},\boldsymbol{x})=\sum_{l_1=0}^{N-1}\sum_{l_2=0}^{N-1}x_{l_2}^*a_{l_2}^*a_{l_1}\chi_{s_{l_1}s_{l_2}}(\tau,f_d)\ . \tag{10}$$

Equation (9) represents the cross-ambiguity function between two chirps of Costas signal; $s_{l_1}(t-l_1\tau_1)$, $s_{l_2}(t-l_2\tau_1)$. We can simplify the equation (8) such that the function $\chi_{MF}(\tau,f_d,\boldsymbol{a},\boldsymbol{x})$ is equal to a sum of two part as follows (Appendix A shows the prove)

$$\chi_{MF}(\tau,f_d,\boldsymbol{a},\boldsymbol{x})=\chi_{MF}^{(ml)}(\tau,f_d,\boldsymbol{a},\boldsymbol{x})+\chi_{MF}^{(sl)}(\tau,f_d,\boldsymbol{a},\boldsymbol{x}), \tag{11}$$

such that the main lobe part is

$$\chi_{MF}^{(ml)}(\tau,f_d,\boldsymbol{a},\boldsymbol{x})=\frac{1}{N}\sum_{l=0}^{N-1}x_l^*|a_l|^2\frac{(\tau_1-|\tau|)}{\tau_1}\mathrm{sinc}\left(\pi f_d(\tau_1-|\tau|)\right)e^{j\pi\kappa_l(\tau,f_d)}:|\tau|\le\tau_1\ , \tag{12}$$

where $\chi_{MF}^{(ml)}(\tau,f_d,\boldsymbol{a},\boldsymbol{x})=0$ for $|\tau|>\tau_1$, and $\kappa_l(\tau,f_d)=-f_d\left((2l+1)\tau_1+\tau\right)+2f_l\tau$.

Again for $|\tau-(l_1-l_2)\tau_1|\le\tau_1$, we get the side lobes part as

$$\chi_{MF}^{(sl)}(\tau,f_d,\boldsymbol{a},\boldsymbol{x})=$$

$$=\frac{1}{N}\sum_{\substack{l_1=0\\ l_2\neq l_1}}^{N-1}\sum_{l_2=0}^{N-1}x_{l_2}^*a_{l_2}^*a_{l_1}\frac{(\tau_1-|\eta_{l_1l_2}(\tau)|)}{\tau_1}\mathrm{sinc}\left(\pi\alpha\left(\tau_1-|\eta_{l_1l_2}(\tau)|\right)\right)e^{j\pi\zeta_{l_1l_2}(\tau,f_d)}, \tag{13}$$

where $\chi_{MF}^{(sl)}(\tau, f_d, \boldsymbol{a}, \boldsymbol{x}) = 0$ for $|\tau - (l_1 - l_2)\tau_1| > \tau_1$, and $\eta_{l_1 l_2}(\tau) = \tau - (l_1 - l_2)\tau_1$, $\zeta_{l_1 l_2}(\tau, f_d) = \alpha(\tau - (l_1 - l_2 - 1)\tau_1) + 2f_{l_2}\eta_{l_1 l_2}(\tau) - 2f_d l_1 \tau_1$, and $\alpha = f_{l_1} - f_{l_2} - f_d$.

We have just modified Woodward's definition of ambiguity in line with our idea that the ambiguity caused by the waveform to the corresponding matched filter output should be taken into account with the inclusion of radar scattering coefficients of the target $\boldsymbol{x}$ and weighted coefficients $\boldsymbol{a}$ of the sent waveform. Hence, being $\chi_{MF}(.)$ in terms of both $\boldsymbol{x}$ and $\boldsymbol{a}$ emphasizes our idea that we could deal with $\boldsymbol{x}$ as the "fingerprint" of the target. For this consideration, the problem of target scattering coefficients estimation must be taken into account, and hence it is important, if our model is applied, to choose a technique for scattering coefficients estimation in the radar system like in [6][19]. However, in simulation we will use Swerling models for estimating the scattering coefficients. The use of both $\boldsymbol{x}$ and $\boldsymbol{a}$ in radar waveform synthesis can be considered as an improvement in the representation of the radar target echo signal in a new ambiguity form defined using Costas encoding in the transmitted waveform. This parametrization is a realistic representation of the signal transmitted and reflected from the radar target, which at the same time allows us to perform an adaptive design of the transmitted Costas waveform. The process begins with assuming a desired AF surface corresponding to some specifications as we will see in **Section 3**.

In the simulation, we do a normalization procedure for our NAF model by computing the ratio $\left|\frac{\chi_{MF}(\tau, f_d, \boldsymbol{a}, \boldsymbol{x})}{\chi_{MF}(0,0,\boldsymbol{a}, \boldsymbol{x})}\right|$, and hence the inequality $0 \le \left|\frac{\chi_{MF}(\tau, f_d, \boldsymbol{a}, \boldsymbol{x})}{\chi_{MF}(0,0,\boldsymbol{a}, \boldsymbol{x})}\right| \le 1$ is satisfied for the entire (τ, f_d)-plane. The purpose of this normalization is to study the volume of the AF surface as unitary quantity.

In the rest of the paper we will consider the magnitude squared $|\chi_{MF}(.)|^2$, as an expression of the NAF surface of a single pulse, because sometimes this expression is referred to as the outputs of an optimum detector filter matched to zero delay (range) and zero Doppler (velocity) according to reference [16], with only the magnitude term of complex two-dimensional function in corresponding equations labeled as the NAF, following the same representation concept of the wideband ambiguity function (WAF) defined in [17].

3. Adaptation Model of Waveform Design

In this section, we propose an adaptation model that adaptively designs the signal proposed in **Section 2**. This adaptation procedure makes the volume of the corresponding NAF of weighted Costas signal best approximates the volume of a desired AF surface. In fact, there are no theoretical techniques known for finding a

waveform corresponding to a desired ambiguity surface, nor is a set of mathematical rules known for ensuring that a desired surface is an AF surface i.e., the waveform that gives rise to this desired surface may not exist. Therefore, by using an optimization approach there might be a waveform with AF surface that is an acceptable approximation to the desired surface.

In fact, the ideal radar waveform would produce an ideal AF equivalent to two-dimensional Dirac delta function on the delay-Doppler plane. Such a function would have ideal range-doppler requirements. However, since no finite energy signal gives rise to ideal AF [2][4], there is a practical reason not to deal with an ideal AF surface somehow in order to get realizable waveforms with some optimal properties. Instead, we can assume that the desired ambiguity function $\chi_{Opt}(\tau, f_d)$ satisfies the following definition

$$\left|\chi_{Opt}(\tau, f_d)\right| = \begin{cases} 1, & (\tau, f_d) = (0,0) \\ 0, & \textit{elsewhere} \end{cases}. \tag{14}$$

By following the optimization approach proposed in [9][13][14], we restrict the optimization procedure over some limited subregions in (τ, f_d)-plane, particularly surrounding the main lobe of the NAF surface. Our goal is to find a waveform that satisfying equation (1) and whose AF surface has desired properties in a certain given subregion of (τ, f_d)-plane. Since the subregions where the volume under AF surface is desired to be small depend on the particular radar application, and in order to give the designer the degree of freedom he desires, the approximation of the AF surface could be developed in any subregion of interest. Hence, our goal is to find a weighted Costas waveform satisfying $\sum_{l=0}^{N-1}|a_l|^2 = 1$, such that the LS error between the volume under the resulting NAF surface $\left|\chi_{MF}(.)\right|^2$ and the volume under desired AF surface $\left|\chi_{Opt}(\tau, f_d)\right|^2$ is minimum. Let $\aleph \subset \mathbb{R}^2$ denotes the subregion of interest such that

$$\aleph = \left\{(\tau, f_d) \in \mathbb{R}^2 : \tau_- \le \tau \le \tau_+, f_- \le f_d \le f_+\right\}. \tag{15}$$

Therefore, finding such an adaptive weights for the Costas waveform is equivalent to find the optimum complex weights $\boldsymbol{a}_{Opt}$ corresponding to the "fingerprint" of the target $\boldsymbol{x}$ such that

$$\boldsymbol{a}_{Opt}(\boldsymbol{x}) = \underset{\boldsymbol{a}}{\operatorname{argmin}} \left\{ \int_{\tau_-}^{\tau_+} \int_{f_-}^{f_+} \left| \left|\chi_{Opt}(\tau, f_d)\right|^2 - \left|\chi_{MF}(\tau, f_d, \boldsymbol{a}, \boldsymbol{x})\right|^2 \right| d\tau df_d \right\}$$

$$\text{subject to } \left(\sum_{l=0}^{N-1} |a_l|^2 = 1 \right) \wedge \left(\forall l \in \{0,1,...,N-1\}; \exists \varepsilon > 0 : |a_l|^2 \ge \varepsilon \right), \tag{P1}$$

where ε is a small positive quantity relatively close to zero ensuring transmission over all N frequency channels of Costas signal, and P1 represents the optimization problem. The reader could note, via P1 formulation, the compatibility of the finding process with the philosophy of "adaptive" design

since $\boldsymbol{a}_{Opt}$ clearly depends on the scattering coefficients of the target x. The optimization algorithm is initialized with fixed weights ($\forall l, a_l = Const$) as an input, then it gives the optimal solution as an output. Performance is measured by comparing the level of side lobes of the matched filter response corresponding to fixed (constant) weights of Costas waveform with the level of side lobes of the response corresponding to the optimal weights. $\sum_{l=0}^{N-1}|a_l|^2 = 1$ and $\forall l, |a_l|^2 \geq \varepsilon$ denote nonlinear constraints needed to have both equality and inequality constraints defined in problem (P1).

In a particular case, when the following inequality holds true at the initialization run time of the optimization algorithm

$$\iint_{\aleph} \left|\chi_{Opt}(\tau, f_d)\right|^2 d\tau df_d \geq \iint_{\aleph} \left|\chi_{MF}(\tau, f_d, \boldsymbol{a}, \boldsymbol{x})\right|^2 d\tau df_d , \tag{16}$$

we can further simplify P1 to the following another one such that

$$\boldsymbol{a}_{Opt}(\boldsymbol{x}) = \underset{\boldsymbol{a}}{\operatorname{argmin}} \left\{ \sum_{l_1=0}^{N-1}\sum_{l_2=0}^{N-1}\sum_{l_3=0}^{N-1}\sum_{l_4=0}^{N-1} a_{l_1} a_{l_2}^* a_{l_3}^* a_{l_4} x_{l_2}^* x_{l_4} \int_{\tau_-}^{\tau_+}\int_{f_-}^{f_+} \chi_{s_{l_1}s_{l_2}}(\tau, f_d)\, \chi_{s_{l_3}s_{l_4}}^*(\tau, f_d) d\tau df_d \right\}$$

$$\text{subject to } \left(\sum_{l=0}^{N-1}|a_l|^2 = 1\right) \wedge \left(\forall l \in \{0,1,...,N-1\}; \exists \varepsilon > 0 : |a_l|^2 \geq \varepsilon\right), \tag{P2}$$

where both $\chi_{s_{l_1}s_{l_2}}(\tau, f_d)$ and $\chi_{s_{l_3}s_{l_4}}(\tau, f_d)$ satisfies the equation (9). In Appendix A, we show that the general formula of $\chi_{s_{l_1}s_{l_2}}(\tau, f_d)$ is proposed by the following

Case 1: when $l_1 = l_2 = l$ and $|\tau| \leq \tau_1$, we get

$$\chi_{s_l s_l}(\tau, f_d) = \frac{1}{N}\frac{(\tau_1 - |\tau|)}{\tau_1}\operatorname{sinc}\left(\pi f_d (\tau_1 - |\tau|)\right) e^{j\pi\kappa_l(\tau, f_d)}, \tag{17}$$

with $\kappa_l(\tau, f_d) = -f_d\left((2l+1)\tau_1 + \tau\right) + 2f_l\tau$.

Case 2: when $l_1 \neq l_2$ and $|\tau - (l_1 - l_2)\tau_1| \leq \tau_1$, we get

$$\chi_{s_{l_1}s_{l_2}}(\tau, f_d) = \frac{1}{N}\frac{\left(\tau_1 - |\eta_{l_1 l_2}(\tau)|\right)}{\tau_1}\operatorname{sinc}\left(\pi\alpha\left(\tau_1 - |\eta_{l_1 l_2}(\tau)|\right)\right) e^{j\pi\xi_{l_1 l_2}(\tau, f_d)}, \tag{18}$$

with $\eta_{l_1 l_2}(\tau) = \tau - (l_1 - l_2)\tau_1$, $\xi_{l_1 l_2}(\tau, f_d) = \alpha\left(\tau - (l_1 - l_2 - 1)\tau_1\right) + 2f_{l_2}\eta_{l_1 l_2}(\tau) - 2f_d l_1 \tau_1$, and $\alpha = f_{l_1} - f_{l_2} - f_d$.

Problems (P1) and (P2) correspond to the NAF of a single weighted Costas pulse; $\chi_{MF}(.)$.

We notice that (P2) leads to a minimization procedure having fourth order form of sums, similar to that presented in [9], where when $l_1 = l_2 = l_3 = l_4 = l$, we have the term $|a_l|^4, \forall l$ which implies nonlinear minimization problem. However, from mathematical point of view, our method can be categorized like [9] as an ℓ_1-

minimization [18] which corresponds to ℓ_1-norm in Hilbert space, while that of [14] as an ℓ_2-minimization which corresponds to ℓ_2-norm in Hilbert space.

However, the convergence time of (P1) , (P2) strongly depends on the area of subregion $\aleph$, and the shape of the desired AF surface; $\left|\chi_{Opt}(\tau, f_d)\right|^2$. If we have a *priori* knowledge of the radar target "fingerprint" $\boldsymbol{x}$, we can use an offline computation of (P1) , (P2) extending over a larger area of $\aleph$, and considering a desired impulse-shaped of the ambiguity surface; $\left|\chi_{Opt}(\tau, f_d)\right|^2$. However, in the situation of an online computation (in real-time processing) of (P1) , (P2) when we need to compute $\boldsymbol{a}_{Opt}$ based on the estimated value of $\boldsymbol{x}$ from the previous radar dwell, it would be practical to restrict $\aleph$ to a smaller region (e.g., $\left\{(\tau, f_d) \in \mathbb{R}^2 : -T \le \tau \le +T,\ -1/(2T) \le f_d \le +1/(2T)\right\}$) and not to choose an "idealistic" shape of the desired ambiguity surface [13][14].

4. Simulation Results and Discussion

Simulation results of the proposed adaptive waveform design are presented in this section. The simulation results verify the effectiveness of the adaptive waveform design in the form of an improved NAF surface corresponding to the optimal weights obtained from the optimization procedure. We assumed that the pulse width of the Costas waveform $T = 7\mu s$, and the hopping sequence of Costas code $c = [4\ 3\ 1\ 2];\ N = 4$.

We evaluated the optimal solution $\boldsymbol{a}_{Opt}$ by using the subregion $\aleph = \left\{(\tau, f_d) \in \mathbb{R}^2 : -T \le \tau \le +T,\ -1/(2T) \le f_d \le +1/(2T)\right\}$) and the desired AF surface $\chi_{Opt}(\tau, f_d)$ matching the inequality (16). We realized the components of $\boldsymbol{x}$ from a *Rayleigh* distribution with average RCS; $\bar{\sigma} = 1m^2$ corresponding to the Swerling I, II models and here we get a realization; $\boldsymbol{x} = [2.1830\ 1.0896\ 2.3444\ 0.8487]$ from MATLAB© random generator. The results $\boldsymbol{a}_{Opt}$ are obtained using a *Constrained Nonlinear Problem Solver* of MATLAB©. We initialized the problem (P1) with $\forall l, a_l = 0.5000$, and $\varepsilon = 0.1$. We demonstrate the advantage of the optimal solution $\boldsymbol{a}_{Opt}$ by comparing adaptively the designed NAF with that obtained from a fixed waveform that employs the initialization considerations of the optimization algorithm (P1). Fig. 1 represents contours plot of normalized main lobe part $\chi_{MF}^{(ml)}$ of NAF of the adaptive waveform (Fig. 1a) comparing with the initial one (Fig. 1b), where the resultant optimal (adaptive) solution is $\boldsymbol{a}_{Opt} = [0.3236\ 0.5776\ 0.3163\ 0.6794]$. Both parts of Fig. 1 cover the normalized delay axis from $-0.8T$ to $0.8T$, and the normalized Doppler axis from $-2/T$ to $2/T$, and the contour lines begin at the level of 0.1 and the spacing between the lines is

also 0.1. It is clear from Fig. 1 that the contours 0.1 to 0.5 of the color-bar are obviously improved. Precisely, the contours 0.4 and 0.5 referring to relatively high sidelobe level and being closer to the main lobe disappeared indicating a considerable reduction in sidelobe levels in the main lobe area of NAF.

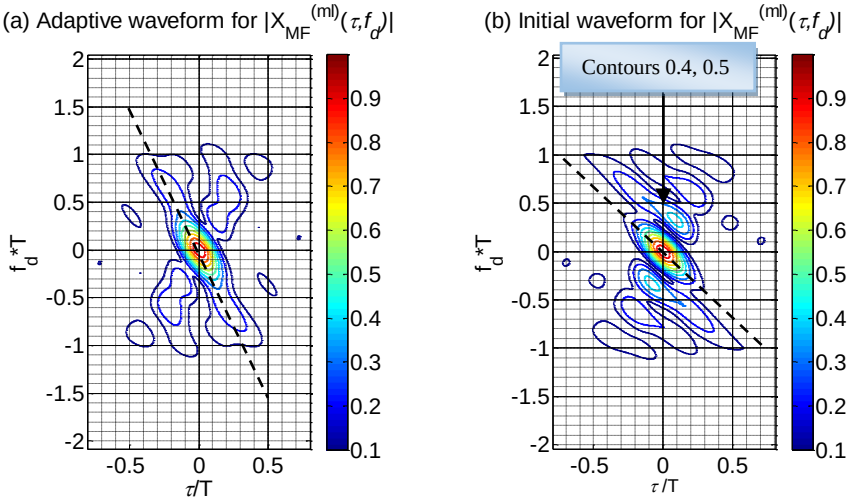

Fig. 1. Contours plot of $\chi_{MF}^{(ml)}(.)$ for (a) Adaptive waveform, and (b) Initial waveform.

In addition, we note, from the diagonal dotted line seen in Fig. 1, that the adaptive waveform yields less sensitivity to delay-Doppler coupling problem, which means that for small Doppler shift; f_d the measured delay location of the improved NAF peak response is shifted from true delay by $\tau_{\text{shift}}^{\text{adaptive}}$ smaller than $\tau_{\text{shift}}^{\text{initial}}$ of the initial NAF. Numerically, the diagonal dotted line slope of the adaptive waveform is about 112^{o} while that of the initial waveform is about 130^{o}, and since the slope is equivalent by analogy to the delay-Doppler coupling coefficient k [1], i.e., $k \propto \left|\tan(slope)\right|$, and from the equation (4.12) of CH 4. in [1] we have $\tau_{\text{shift}} = f_d / k$, so we get $\tau_{\text{shift}}^{\text{adaptive}} = \tau_{\text{shift}}^{\text{initial}} / 2.1$ for same small Doppler shift.

Fig. 2. shows the zero-Doppler cut plot of NAF (i.e., ACF). According to Fig. 2.a, we could emphasize that the adaptive waveform results in a very much better ACF, where the first sidelobe level of the normalized NAF corresponding to the adaptive waveform is less than the one of the fixed waveform by 36.3 times (linear scale), which means that it is attenuated by 15.6 dB as Fig. 2.b shows. These results confirm the validity of our adaptive waveform design, where we achieved about 15.6 dB in reducing the PSL of ACF (i.e., the PSL of the AF at zero Doppler cut).

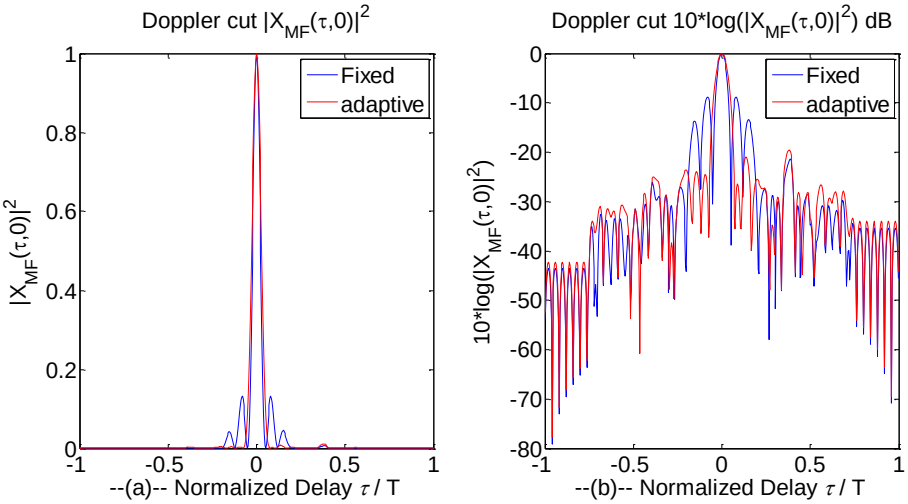

Fig. 2. Zero-Doppler cuts (ACF) of the NAF corresponding to the adaptive and fixed waveforms, (a) linear scale, (b) in dB.

Fig. 2. also suggests that there is no important change in the nominal delay resolution, and hence we conclude that our model yields very good reduction in PSL of ACF without any important change in the delay resolution.

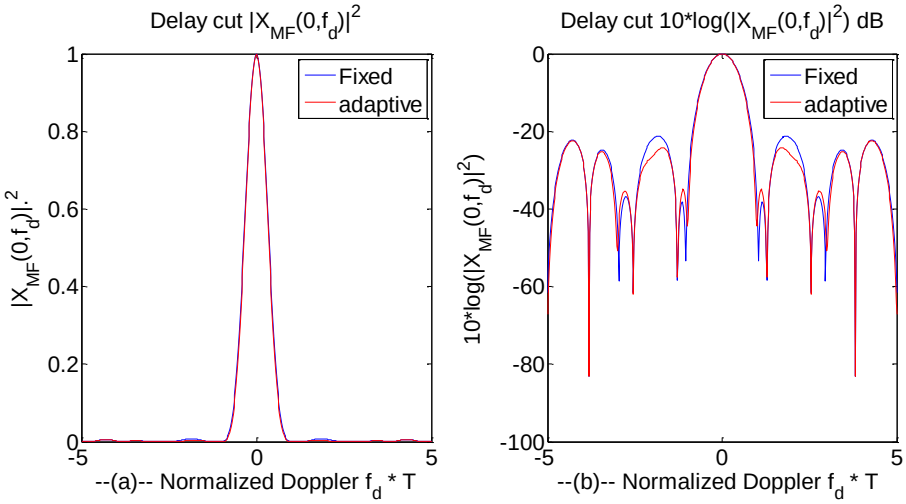

Fig. 3. Zero-delay cuts of the NAF corresponding to the adaptive and fixed waveforms, (a) linear scale, (b) in dB.

Fig. 3. shows the zero-delay cut plot of the NAF obtained in the simulation. As we expect, there is no important change neither in the PSL value nor in the Doppler resolution as Fig. 3 indicates. Precisely, the reduction in PSL is attenuated by about just 3 dB. We checked our model over 25 independent realizations of scatters coefficients, and always we got similar results.

We interpret our results by looking into the energy distributions of the adaptive waveform and the target response over the four different subcarriers $\{f_l\}_{0\le l\le 4}$. Since the variance of $|\boldsymbol{a}.\boldsymbol{x}|$ obtained in our simulation is reduced from $\mathrm{var}\left(|\boldsymbol{a}_{Fix}.\boldsymbol{x}|\right)=0.1432$ to $\mathrm{var}\left(\left|\boldsymbol{a}_{Opt}.\boldsymbol{x}\right|\right)=0.0055$ meaning that the amplitude of the target echo is approximately constant, we could say that the signal energy redistributes its ell such that more signal energy must be supplied to a particular subcarrier in which the target response is weaker, where the chirp ,in this case, is f_3 and this subcarrier corresponds to the weakest scatter $x_3=0.8487$, and hence the radar system needs to make the weight $a_3=0.6794$ be the largest one as obtained in our minimization procedure. On the other hand, less signal energy should be supplied to the subcarriers over which the target response is already stronger, where the chirps ,in this case, are f_0, f_2 that correspond to two strongest scatters $x_0=2.1830, x_2=2.3444$, and hence the radar system needs to make the weights $a_0=0.3236, a_2=0.3163$ be the smallest ones in $\boldsymbol{a}_{Opt}$ which was achieved. Furthermore, the scatter $x_1=1.0896$ corresponding to the subcarrier f_1 is approximately equal to unity, so the weight of the corresponding chirp in Costas signal should not be much different from the original fixed one in the fixed waveform (no actual change in supplied energy is required), and for this reason the minimization procedure resulted in the value $a_1=0.5776$ in $\boldsymbol{a}_{Opt}$ such that it is approximately equal to 0.5000 as it was in the vector $\boldsymbol{a}_{Fix}$. Finally, it is clear for the reader that the adaptive waveform obtained in our simulation does not satisfy the common requirement of constant amplitude in radar signal in which transmitting tubes operate most under constant-amplitude conditions [3], but since the variance of the optimal solution $\mathrm{var}\left(\boldsymbol{a}_{Opt}\right)=0.0335$ is relatively small, we could accept these relatively small variations in amplitude of the resultant Costas chirps. As a future work, we could add a linear constraint and a nonlinear constraint to the optimization procedures (P1) , (P2) presented in this paper so that the average of $\boldsymbol{a}$; $\bar{\boldsymbol{a}}=\frac{1}{N}\sum_{l=0}^{N-1}|a_l|$, and the variance of $\boldsymbol{a}$ **;** $\sigma_{\boldsymbol{a}}^2=\frac{1}{N}\sum_{l=0}^{N-1}\left(|a_l|-\bar{\boldsymbol{a}}\right)^2$ are statistically acceptable values under transmitting tubes operation requirements. However, the resultant adaptive waveform in this study exhibits very good ambiguity behavior in subregion surrounding the main lobe in the sense of PSL, and does not really influence the Delay-Doppler resolution, and without needing to increase *N*.

5. Conclusions

We developed a new Costas waveform including adaptive weights corresponding to scattering coefficients of the target fluctuating according to one

of the Swerling models, with acceptable variations in amplitude of the resulting Costas chirp signal. We computed the NAF formula of this waveform. We formulated the radar waveform optimization problem to result in those adaptive weights such that its solution minimizes the volume under the corresponding NAF surface in comparison with the volume under desired NAF surface in the LS sense. We emphasized that the adaptive waveform results in much ACF where the PSL of ACF of the improved NAF corresponding to the adaptive waveform is attenuated by 15.6 dB with respect to the PSL of ACF corresponding to the fixed waveform. Our model yields very good PSL reduction without change in delay resolution, so much better detection performance. There also was no important change neither in the PSL of the NAF delay cut, nor in Doppler resolution. Moreover, the adaptive waveform yields less sensitivity to delay-Doppler coupling problem. We interpreted our results in the sense of energy redistribution at the scatters of the target, where the weaker scatter should be supplied with more energy than the stronger one. We are currently preparing a paper to formulate and calculate the NAF model of a coherent pulse train of weighted Costas pulses and show if the same results could be obtained and even improved. In future work, we aim to generalize our model by applying variable time spacing between the subcarriers of Costas array such that the time spacing between sub-pulses of Costas signal changes over all N weighted frequency channels. In addition, we aim to test the proposed adaptive design model through field experiments to make measurements on a real possible target in a reverberation chamber.

Appendix A

We could rewrite the equation (8) such that

$$\chi_{MF}(\tau,f_d,\boldsymbol{a},\boldsymbol{x}) = \frac{1}{N\tau_1}\sum_{l=0}^{N-1} x_l^* |a_l|^2 \int_{-\infty}^{+\infty} s_l(t-l\tau_1)s_l^*(t-\tau-l\tau_1)e^{-j2\pi f_d t}dt + \frac{1}{N\tau_1}\sum_{l_1=0}^{N-1}\sum_{\substack{l_2=0 \\ l_2\neq l_1}}^{N-1} x_{l_2}^* a_{l_2}^* a_{l_1} \int_{-\infty}^{+\infty} s_{l_1}(t-l_1\tau_1)s_{l_2}^*(t-\tau-l_2\tau_1)e^{-j2\pi f_d t}dt \quad , \tag{A1}$$

and define

$$\Phi_{ll}(\tau,f_d) = \frac{1}{\tau_1}\int_{-\infty}^{+\infty} s_l^*(t-l\tau_1)s_l(t-\tau-l\tau_1)e^{+j2\pi f_d t}dt \ , \tag{A2}$$

$$\Phi_{l_1l_2}(\tau,f_d) = \frac{1}{\tau_1}\int_{-\infty}^{+\infty} s_{l_1}^*(t-l_1\tau_1)s_{l_2}(t-\tau-l_2\tau_1)e^{+j2\pi f_d t}dt : l_1\neq l_2 \ . \tag{A3}$$

We notice that

$$\frac{1}{\tau_1}\int_{-\infty}^{+\infty} s_l(t-l\tau_1)s_l^*(t-\tau-l\tau_1)e^{-j2\pi f_d t}dt = \Phi_{ll}^*(\tau,f_d) \ , \tag{A4}$$

$$\frac{1}{\tau_1}\int_{-\infty}^{+\infty} s_{l_1}(t-l_1\tau_1)s_{l_2}^*(t-\tau-l_2\tau_1)e^{-j2\pi f_d t}dt = \Phi_{l_1l_2}^*(\tau,f_d) : l_1\neq l_2 \ . \tag{A5}$$

By changing the variable in (A.4) such that $\sigma = t - l\tau_1$ we get

$$\Phi_{ll}(\tau, f_d) = e^{+j2\pi f_d l\tau_1} \frac{1}{\tau_1} \int_{-\infty}^{+\infty} s_l^*(\sigma) s_l(\sigma - \tau) e^{+j2\pi f_d \sigma} d\sigma = e^{+j2\pi f_d l\tau_1} \phi_{ll}(\tau, f_d), \quad \text{(A6)}$$

where $\phi_{ll}(\tau, f_d) = \frac{1}{\tau_1} \int_{-\infty}^{+\infty} s_l^*(\sigma) s_l(\sigma - \tau) e^{+j2\pi f_d \sigma} d\sigma$. (A7)

In fact, equation (A7) represents the autocorrelation function of $s_l(t)$ (one of the Costas chirps), and is simplified directly by using the Costas calculation corresponding to equation (21) of his original paper [15], so we get

$$\phi_{ll}(\tau, f_d) = \begin{cases} \frac{(\tau_1 - |\tau|)}{\tau_1} \operatorname{sinc}\left(\pi f_d (\tau_1 - |\tau|)\right) e^{\left[j\pi f_d (\tau_1 + \tau) - j2\pi f_l \tau\right]}, & |\tau| \le \tau_1 \\ 0, & \textit{elsewhere} \end{cases} \quad \text{(A8)}$$

Substituting (A8) into (A6), we get

$$\Phi_{ll}(\tau, f_d) = \begin{cases} \frac{(\tau_1 - |\tau|)}{\tau_1} \operatorname{sinc}\left(\pi f_d (\tau_1 - |\tau|)\right) e^{\left[j\pi f_d ((2l+1)\tau_1 + \tau) - j2\pi f_l \tau\right]}, & |\tau| \le \tau_1 \\ 0, & \textit{elsewhere} \end{cases} \quad \text{(A9)}$$

We put $\kappa_l(\tau, f_d) = -f_d((2l+1)\tau_1 + \tau) + 2f_l\tau$, then substituting (A9) into (A4), we get

$$\frac{1}{\tau_1} \int_{-\infty}^{+\infty} s_l(t - l\tau_1) s_l^*(t - \tau - l\tau_1) e^{-j2\pi f_d t} dt = \begin{cases} \frac{(\tau_1 - |\tau|)}{\tau_1} \operatorname{sinc}\left(\pi f_d (\tau_1 - |\tau|)\right) e^{j\pi\kappa_l(\tau, f_d)}, & |\tau| \le \tau_1 \\ 0, & \textit{elsewhere} \end{cases} . \quad \text{(A10)}$$

Then, substituting (A10) into the first term of (A1) with $|\tau| \le \tau_1$, we get the main lobe ambiguity function

$$\chi_{MF}^{(\mathrm{ml})}(\tau, f_d, \boldsymbol{a}, \boldsymbol{x}) = \frac{1}{N} \sum_{l=0}^{N-1} x_l^* |a_l|^2 \frac{(\tau_1 - |\tau|)}{\tau_1} \operatorname{sinc}\left(\pi f_d (\tau_1 - |\tau|)\right) e^{j\pi\kappa_l(\tau, f_d)}, \quad \text{(A11)}$$

and $\chi_{MF}^{(\mathrm{ml})}(\tau, f_d, \boldsymbol{a}, \boldsymbol{x}) = 0$ elsewhere. Hence, this is corresponding to equation (12).

By changing the variable in (A3) such that $\sigma = t - l_1\tau_1$ remembering in this case that $l_1 \ne l_2$, we get

$$\Phi_{l_1 l_2}(\tau, f_d) = e^{+j2\pi f_d l_1\tau_1} \frac{1}{\tau_1} \int_{-\infty}^{+\infty} s_{l_1}^*(\sigma) s_{l_2}(\sigma + (l_1 - l_2)\tau_1 - \tau) e^{+j2\pi f_d \sigma} d\sigma . \quad \text{(A12)}$$

By changing the variable in (A.12) such that $\tau' = \tau - (l_1 - l_2)\tau_1$, we get

$$\Phi_{l_1 l_2}(\tau' + (l_1 - l_2)\tau_1, f_d) = e^{+j2\pi f_d l_1\tau_1} \frac{1}{\tau_1} \int_{-\infty}^{+\infty} s_{l_1}^*(\sigma) s_{l_2}(\sigma - \tau') e^{+j2\pi f_d \sigma} d\sigma = e^{+j2\pi f_d l_1\tau_1} \phi_{l_1 l_2}(\tau', f_d) \quad \text{(A13)}$$

where we put

$$\phi_{l_1 l_2}\left(\tau^{'}, f_d\right) = \frac{1}{\tau_1}\int_{-\infty}^{+\infty} s_{l_1}^{*}(\sigma) s_{l_2}\left(\sigma - \tau^{'}\right) e^{+j\,2\pi f_d \sigma} d\,\sigma\,. \tag{A14}$$

In fact, the equation (A14) represents the cross-correlation function between two Costas chirps $s_{l_1}(t), s_{l_2}(t)$ and is simplified directly by using the Costas calculation corresponding to equation (18) of his original paper in [15], so we get

$$\phi_{l_1 l_2}\left(\tau^{'}, f_d\right) = \begin{cases} \dfrac{\left(\tau_1 - \left|\tau^{'}\right|\right)}{\tau_1} \operatorname{sinc}\left(\pi\alpha\left(\tau_1 - \left|\tau^{'}\right|\right)\right) e^{\left[-j\,\pi\alpha\left(\tau_1+\tau^{'}\right) - j\,2\pi f_{l_2}\tau^{'}\right]}, & \left|\tau^{'}\right| \le \tau_1\,, \\ 0, & \textit{elsewhere} \end{cases} \tag{A15}$$

where $\alpha = f_{l_1} - f_{l_2} - f_d$ is corresponding to equation (20) in [15]. Substituting (A15) into (A13) and returning to the variable τ, we get for $\left|\tau^{'}\right| \le \tau_1$

$$\begin{aligned} &\phi_{l_1 l_2}\left(\tau^{'}, f_d\right) = \phi_{l_1 l_2}\left(\tau - \left(l_1 - l_2\right)\tau_1, f_d\right) = \\ &= \frac{\left(\tau_1 - \left|\tau - \left(l_1 - l_2\right)\tau_1\right|\right)}{\tau_1} \operatorname{sinc}\left(\pi\alpha\left(\tau_1 - \left|\tau - \left(l_1 - l_2\right)\tau_1\right|\right)\right) e^{\left[-j\,\pi\alpha\left(\tau - (l_1 - l_2 - 1)\tau_1\right) - j\,2\pi f_{l_2}\left(\tau - (l_1 - l_2)\tau_1\right)\right]}, \end{aligned} \tag{A16}$$

$\phi_{l_1 l_2}\left(\tau^{'}, f_d\right) = 0$ elsewhere. If we put $\eta_{l_1 l_2}(\tau) = \tau - \left(l_1 - l_2\right)\tau_1$, and $\zeta_{l_1 l_2}(\tau, f_d) = \alpha\left(\tau - \left(l_1 - l_2 - 1\right)\tau_1\right) + 2 f_{l_2}\eta_{l_1 l_2}(\tau) - 2 f_d l_1 \tau_1$, and substituting (A16) into (A13), we get

$$\begin{aligned} &\Phi_{l_1 l_2}\left(\tau^{'}, f_d\right) = e^{+j\,2\pi f_d l_1 \tau_1} \phi_{l_1 l_2}\left(\tau^{'}, f_d\right) = \\ &= \begin{cases} \dfrac{\left(\tau_1 - \left|\eta_{l_1 l_2}(\tau)\right|\right)}{\tau_1} \operatorname{sinc}\left(\pi\alpha\left(\tau_1 - \left|\eta_{l_1 l_2}(\tau)\right|\right)\right) e^{-j\,\pi\,\zeta_{l_1 l_2}(\tau, f_d)}, & \left|\tau^{'}\right| \le \tau_1\,. \\ 0, & \textit{elsewhere} \end{cases} \end{aligned} \tag{A17}$$

Substituting (A17) into (A5), we get

$$\begin{aligned} &\frac{1}{\tau_1}\int_{-\infty}^{+\infty} s_{l_1}\left(t - l_1\tau_1\right) s_{l_2}^{*}\left(t - \tau - l_2\tau_1\right) e^{-j\,2\pi f_d t} dt = \\ &== \begin{cases} \dfrac{\left(\tau_1 - \left|\eta_{l_1 l_2}(\tau)\right|\right)}{\tau_1} \operatorname{sinc}\left(\pi\alpha\left(\tau_1 - \left|\eta_{l_1 l_2}(\tau)\right|\right)\right) e^{+j\,\pi\,\zeta_{l_1 l_2}(\tau, f_d)}, & \left|\tau^{'}\right| \le \tau_1 \\ 0, & \textit{elsewhere} \end{cases}. \end{aligned} \tag{A18}$$

Then, substituting (A.18) into the second term of (A.1) with $\left|\tau - \left(l_1 - l_2\right)\tau_1\right| \le \tau_1$ we get the side lobe ambiguity function

$$\begin{aligned} &\chi_{MF}^{(sl)}\left(\tau, f_d, \boldsymbol{a}, \boldsymbol{x}\right) = \\ &= \frac{1}{N}\sum_{l_1=0}^{N-1}\sum_{\substack{l_2=0 \\ l_2 \ne l_1}}^{N-1} x_{l_2}^{*} a_{l_2}^{*} a_{l_1} \frac{\left(\tau_1 - \left|\eta_{l_1 l_2}(\tau)\right|\right)}{\tau_1} \operatorname{sinc}\left(\pi\alpha\left(\tau_1 - \left|\eta_{l_1 l_2}(\tau)\right|\right)\right) e^{\,j\,\pi\,\zeta_{l_1 l_2}(\tau, f_d)}\,, \end{aligned} \tag{A19}$$

and $\chi_{MF}^{(\mathrm{sl})}\left(\tau, f_d, \boldsymbol{a}, \boldsymbol{x}\right) = 0$ elsewhere. Hence, this is corresponding to equation (13).

We get the formula of equation (11) by substituting (A11) and (A19) in (A1). Finally, the case 1 (equation (17)) in **Section 3** is corresponding to equation (A10), while the case 2 (equation (18)) is corresponding to equation (A18).

R E F E R E N C E S

[1]. *Levanon, Nadav, and Eli Mozeson. Radar Signals. Wiley, 2004*

[2]. *M. I. Skolnik,* Introduction to Radar Systems, 2nd ed. New York: McGraw-Hill, 1980

[3]. *A. W. Rihaczek,* Principles of High-Resolution Radar. New York: McGraw-Hill, 1969

[4]. *N. Levanon,* Radar Principles. New York: Wiley-Interscience, 1988

[5]. *Wei Fu, Defu Jiang, Yiyue Gao, Na Li,* Adaptive optimal waveform design algorithm based on frequency-stepped chirp signal, IET Radar Sonar Navig, **vol. 13**, no. 6, 2019, pp. 892-899

[6]. *Peng Chen, Chenhao Qi, Lenan Wu, Xianbin Wang,* Waveform Design for Kalman Filter-Based Target Scattering Coefficient Estimation in Adaptive Radar System, IEEE Transactions on Vehicular Technology, **vol. 67**, no. 12, 2018, pp. 11805-11817

[7]. *D. A. Hague,* Optimal waveform design using Multi-Tone Sinusoidal Frequency Modulation, OCEANS 2017 - Anchorage, Anchorage, AK, USA, 2017, pp. 1-6

[8]. *Xiongjun Fu, Shuilian Peng, Chengyan Zhang, Min Xie* and *L. P. Ligthart,* Optimal waveform synthesis for adaptive radar, 2016 IEEE International Conference on Signal Processing, Communications and Computing (ICSPCC), Hong Kong, 2016, pp. 1-6

[9]. *S. Sen and A. Nehorai,* Adaptive design of OFDM radar signal with improved wideband ambiguity function, IEEE Transactions on Signal Processing, **vol. 58**, no. 2, 2010, pp. 928-933

[10]. *P. M. Woodward,* Probability and Information Theory, With Applications to Radar. New York: McGraw-Hill, 1953

[11]. *Calvin H. Wilcox,* The synthesis problem for radar ambiguity functions. In: *Richard E. Blahut, Willard Miller, Jr., Calvin H. Wilcox,* editors. Radar and Sonar Part I, Springer-Verlag New York, Inc. The IMA Volumes in Mathematics and its Applications, **vol. 32**, 1991, pp. 229–260

[12]. *S. Sussman,* Least-square synthesis of radar ambiguity functions, IRE Trans. Inf. Theory, **vol. 8**, no. 3, Apr. 1962, pp. 246–254

[13]. *I. Gladkova, D. Chebanov, "*On a new extension of Wilcox 's method*,"* in Proc. 5th WSEAS, Int. Conf. Appl. Math.; Miami, FL, 2004, pp.1-6

[14]. *I. Gladkova and D. Chebanov,* On the synthesis problem for a waveform having a nearly ideal ambiguity surface, presented at the 2004 Int. Radar Conf., Toulouse, France, Oct. 18–22, 2004

[15]. *Costas, J.P.,* A study of a class of detection waveforms having nearly ideal range; doppler ambiguity properties, Proceedings of the IEEE, **vol. 72**, no. 8, Aug.1984, pp. 996–1009

[16]. *J.-C. Guey, M. R. Bell,* Diversity waveform sets for delay-Doppler imaging, IEEE Trans. Inf. Theory, **vol. 44**, no. 4, Jul. 1998, pp. 1504–1522

[17]. *Cristina Soviany,* Embedding Data and Task Parallelism in Image Processing Applications, PhD Thesis, Technische Universiteit Delft, 2003

[18]. *Holger Rauhut, Rachel Ward,* Interpolation via weighted ℓ1 minimization, Applied and Computational Harmonic Analysis, **vol. 40**, no. 2, 2016, pp. 321-351

[19]. *Chen Peng, and Lenan Wu.* Target Scattering Coefficients Estimation in Cognitive Radar under Temporally Correlated Target and Multiple Receive Antennas Scenario. IEICE Transactions on Communications, **vol. E98.B**, no. 9, 2015, pp. 1914–1923